Planar Magnetic Colloidal Crystals

Weijia Wen, Lingyun Zhang, and Ping Sheng

Department of Physics, The Hong Kong University of Science and Technology, Clear Water Bay, Kowloon, Hong Kong, China
(Received 14 June 2000)

We report a novel form of planar magnetic colloidal crystals formed by coated magnetic microspheres floating on a liquid meniscus. Under an external magnetic field, the balance between the repulsive magnetic interaction and the "attractive" interaction, due to the weight of the particles projected along the surface tangent, yields not only the triangular lattice with a variable lattice constant, but also all the other planar crystal symmetries such as the oblique, centered-rectangular, rectangular, and square lattices. By using two different sized magnetic particles, local formations of 2D quasicrystallites with fivefold symmetry are also observed.

Since its discovery more than two decades ago, colloidal crystals have blossomed into a fertile area of research encompassing diverse approaches for controlled fabrication of three-dimensional mesocrystals, i.e., crystals with lattice constants ranging from submicrons to tens of microns [1–11]. More recently, two-dimensional, or planar, colloidal crystals have been observed through a number of self-assembly techniques such as magnetic hole formed with nonmagnetic particles in a ferrofluid [12], field-induced assembly of floating magnetic particles [13], electric-field-induced planar crystal [14], and surfactant-mediated colloid crystals [15]. In particular, two-dimensional magnetic colloidal crystals have afforded fundamental studies on 2D melting and crystallization, mediated with the hexatic phase [16].

In this Letter, we report the unexpected discovery that in a certain parameter range of monodispersed magnetic particles, two-dimensional (2D) crystals can be formed on a fluid surface with not just the (hexagonal) triangular lattice, but also with all the other planar crystal symmetries such as the oblique, centered-rectangular, rectangular, and square lattices [17]. These lattice structures, some of which are metastable, can be reversibly tuned by adjusting the polar and azimuthal angles of the magnetic field relative to the surface normal and the symmetry direction of the 2D lattices. Furthermore, by using two different sized magnetic particles, local formations of 2D quasicrystallites with fivefold symmetry were observed. Theoretical predictions based on energy considerations are shown to be in good agreement with the experiments.

The spherical magnetic particles are fabricated by coating $52(\pm 2)$-μm and $26(\pm 2)$-μm-sized glass spheres with ~ 2-μm and 1.5-μm-thick nickel layers, respectively. In order to obtain magnetic microspheres with controllable moments, we selected uniform glass microspheres with two different sizes as the initial cores and coated a thin layer of nickel using the electroless plating technique [18]. The nickel-coated microspheres were heated in a vacuum chamber at 400 °C for 2 h and then annealed at 550 °C for 3 h. The annealed microspheres possess a small magnetic moment, on the order of 10^{-6} emu for the larger

spheres [19]. The scanning electron microscope images indicate the Ni coating to be uniformly deposited, shown in the lower inset in Fig. 1. Planar colloidal crystals were formed by dispersing 52-μm-sized coated microspheres on the surface of glycerin, contained in a glass bottle with a diameter of 1 cm. The bottle was placed in a rotatable aluminum stage located in the center region of a pair of Holmholz coils, where the magnetic strength of coils was adjusted by a computer-controlled current source. In order to change direction of magnetic field relative to the liquid surface, the Helmholz coil can rotate freely along its diameter. Lattice formation and transitions were monitored and recorded by a video system.

In the absence of a magnetic field, the coated microspheres aggregate in the center region of the slightly curved liquid surface, visible in the upper inset in Fig. 1. When a perpendicular magnetic field was applied, the spheres move radially outward and form a stable hexagonal lattice. The entire process of hexagonal lattice formation is shown in the lower insets in Fig. 1, where the lattice constant is noted to increase monotonically as a function of the field strength. This behavior clearly indicates a competition between the repulsive magnetic interaction and the "attractive" interaction due to the weight of the particles projected along the surface tangent. Such competition is possible because the attractive and repulsive interactions are on the same order due to the fact that the magnetic interaction, which depends on the coating thickness, and the weight of the sphere, which depends on the sphere diameter, can be separately controlled in our system. Quantitative predictions based on this simple picture, given below, are shown to give excellent agreement with the experiment.

By using the boundary condition and the Laplace formula, the shape of surface can be deduced as $z = z_0\{[I_0(\lambda r) - 1]/[I_0(\lambda r_0) - 1]\}$, where z denotes the surface height, with $z = 0$ at the center of the surface $r = 0$, $I_0(x)$ is the zeroth order modified Bessel function of the first kind, $\lambda = \sqrt{\rho_\ell g/\sigma}$, where $\rho_\ell = 1.26 \times 10^3$ kg/m^3 denotes the mass density of glycerin, g denotes the gravitational acceleration, and $\sigma = 63.4$ mJ/m^2 denotes the surface tension. Here the maximum depth of liquid
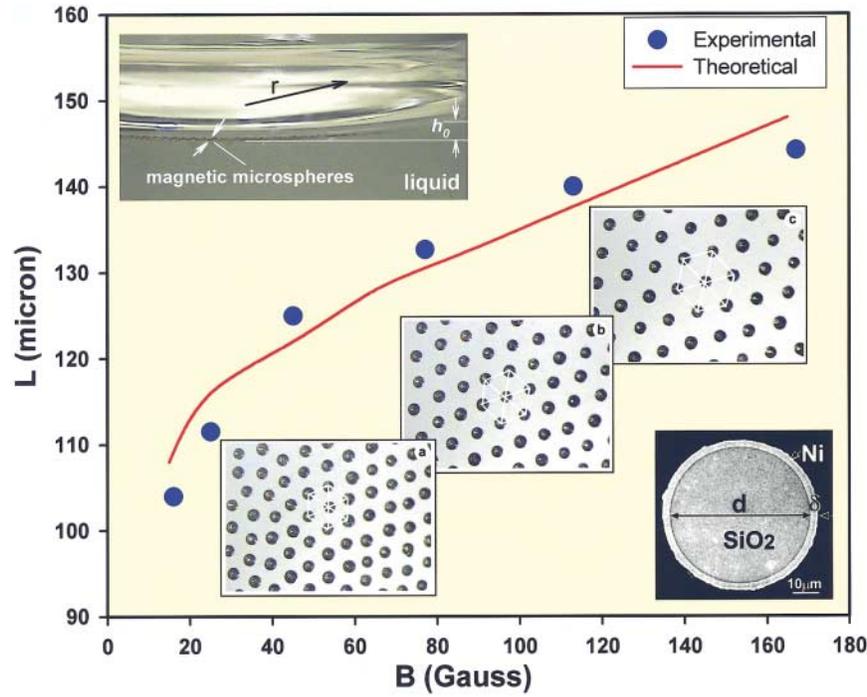
FIG. 1 (color). Variation of the hexagonal lattice constant as a function of the external field. Solid line is theory: solid circles denote measured values. Pictures of the hexagonal lattice under (a) 17 G, (b) 28 G, and (c) 80 G. A cross-sectional picture of the coated sphere is shown in the lower-right inset. The curved liquid meniscus is shown in the upper-left inset.

surface, z_0, and the radius of the container $r_0 = 0.5$ cm are given experimentally. The maximum height z_0 is noted to depend on the weight of the coated spheres. Its value can be measured by photographical means. A picture of the curved fluid surface is shown in the upper inset in Fig. 1.

The magnetostatic energy density U_m consists of the energy of magnetic dipole-dipole interaction and the external field,

$$U_m = \frac{1}{\Omega} \left(\sum_{i<j} \frac{\vec{u}_i \cdot \vec{u}_j}{r_{ij}^3} - 3 \frac{(\vec{u}_i \cdot \vec{r}_{ij})(\vec{u}_j \cdot \vec{r}_{ij})}{r_{ij}^5} - \sum_i \vec{h} \cdot \vec{u}_i \right), \qquad (1)$$

where $\vec{u}_i = \vec{m}_i + \chi \vec{h}$ is the total magnetic dipole moment at site i, $\vec{m}_i$ is the permanent dipole moment of sphere i, χ is the magnetic susceptibility, and $\vec{h}$ is the external field. Here $\vec{r}_{ij}$ denotes the vector pointing from the position of the ith dipole to that of the jth dipole. To find the equilibrium orientation state of the dipoles, we start from different initial random configurations and use dissipative spin dynamics to evolve towards the configuration of minimum energy. When the magnetic energy is considered together with the gravitational potential of the microspheres on the fluid surface, the lattice structure and the lattice constant are determined by the condition of minimum total energy. This is so because the thermal effect is totally negligible in our system due to the size of the microspheres. The results of our calculations show the triangular lattice to

be the most favorable for normal applied field. The predicted lattice constant variation as a function of the applied field is in good agreement with the experiment, as shown in Fig. 1. Here the only parameters involved are $|\vec{m}| \sim 10^{-6}$ emu and $\chi \sim 0.008$, both estimated from experimental and material parameters, e.g., nickel's magnetization of 55 emu/g.

Structural transitions were realized by tilting the magnetic field at an angle θ away from the z direction and rotating an angle ϕ relative to the x axis as defined in the upper inset in Fig. 2. A pictorial summary of all the different structures observed, and their occurrence in the θ, ϕ coordinates, is shown in Fig. 2. With increasing θ and fixed $\phi = 0$, the lattice constant along the x axis decreases while that along the y direction increases to form the centered rectangular structure, as shown in Fig. 2(c). Starting at $\theta = 27°$, lattice instability sets in. Some of the spheres are attracted by their neighbors to form short chains as indicated by the arrows in Fig. 2(d). Further increase in θ leads to perfectly equally spaced, straight chains aligned along the field direction, as shown in Fig. 2(f). Besides the equal spacing, it is noteworthy that the neighboring chains are also shifted by half a diameter in respect to each other.

To obtain other planar crystal structures, we start from the case shown in Fig. 2(b) and then rotate the center stage holder along the φ direction. If the rotation is very slow, e.g., less than a few degrees per minute, then the whole pattern would just rotate in step with the magnetic field, and there is no change in the lattice structure. However,
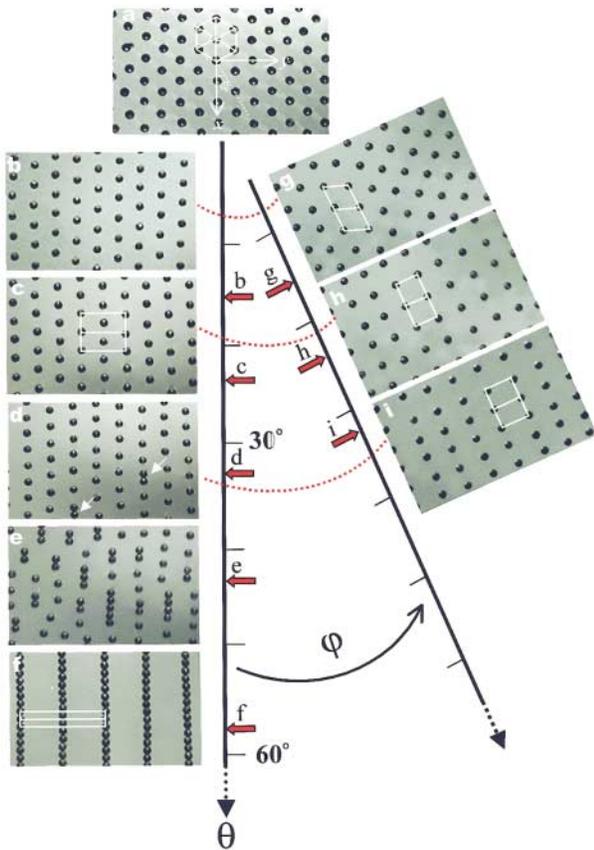
FIG. 2 (color). The formation of different planar lattice structures along the polar angle θ, shown increasing downward, and the azimuthal angle ϕ of the magnetic field. Here the z axis is the surface normal at the center of the liquid meniscus, and the x axis is defined in the uppermost picture.

a rotation rate faster than $1°/s$, for example, would result in structure change. These facts indicate a long relaxation time for the observed structures. By rotating at a rate of about $2°/s$ to $\varphi = 20°$, a planar oblique structure is observed, as shown in Fig. 2(g). The square and rectangular planar structures are obtained by starting either from (c) and (d) and then rotating along the ϕ direction to (h) and (i), respectively, or by starting from (g) and further rotating along the θ direction. These structures are metastable, in the sense that if strongly perturbed, they would go back to the $\phi = 0$ states. Nevertheless, all planar structures can be obtained uniquely and repeatably as a function of θ and ϕ.

The lattice instability starting at $\theta = 27°$ is instrumental for all the lattice structures formed subsequently. Its origin may be traced to a cooperative dipole rotation, which can be predicted theoretically as well as visualized experimentally. In Fig. 3, the respective energies of three lattice structures—hexagonal, centered-rectangular, and chain—are shown. At points a and b, indicated by arrows, the energy curves cross, implying structural transitions should occur at $22°$ (from hexagonal to centered-rectangular) and $55°$ (to the chain structure). These values are in excel-
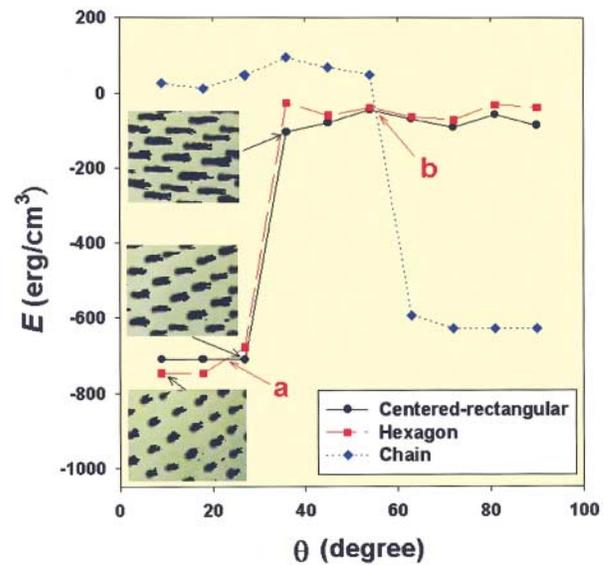
FIG. 3 (color). Calculated total energies of three different planar structures. The crossing points, denoted a and b, are the θ values at which the structural transitions occur. They are in excellent agreement with the experiment. The insets give a direct visualization of the cooperative dipole rotation associated with the increase in total energies.

lent agreement with the experimentally measured values of $23°$ and $57°$, respectively. The large increase in the energies following the $23°$ transition is due to the cooperative rotation of the magnetic dipoles from a predominantly vertical orientation to a predominantly flat orientation. By defining an order parameter, $S = \langle M \rangle = \sum_i m_{iz}/N$, for the spin magnetization component along the vertical direction, this cooperative rotation of the dipole orientation can be easily quantified to vary from $S = 0.9$ at $\theta = 27°$ to $S = 0.07$ at $\theta = 36°$. However, perhaps more interesting is the direct visualization of this dipole rotation. This was realized by dispersing nanosized nickel particles on each sphere. These nanoparticles would tend to aggregate at the magnetic poles. Under a vertical magnetic field, the nanoparticles project upward, shown in the lower-left inset in Fig. 3. When the dipoles are rotated, the nanoparticles form an elongated steak aligned along the in-plane projection of the local magnetic field, shown in the two upper-left insets in Fig. 3.

By mixing the 52- and 26-μm-sized spheres in a ratio of 4:1, we found that in most cases, a small sphere is surrounded by five large spheres to form a five-sided local formation under a vertical magnetic field. The overall structure is amorphous. However, we have unexpectedly found that in some areas there can be beautiful textbook examples of quasicrystal formations with fivefold rotational symmetry, as shown in Fig. 4. To our knowledge, this is the first time that such a 2D pattern has been reproduced as a force-balanced, natural-occurring metastable state.

We have demonstrated that by using coated spheres with weak magnetic moments, many different forms of planar
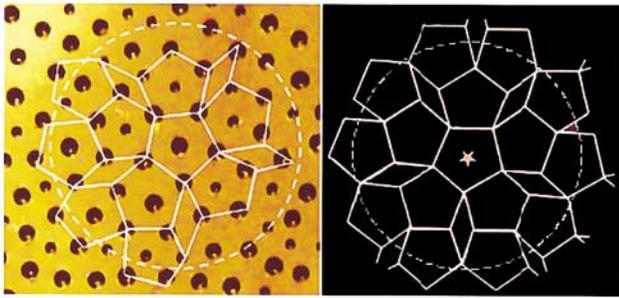
FIG. 4 (color). Left panel: a picture of the locally fivefold symmetric structure observed at one area of the overall amorphous planar lattice with two different sized coated microspheres. There is an imperfection in the structure, at about the 7 o'clock position, where a large sphere is located at the position for a small sphere. Right panel: a drawing of a fivefold quasicrystalline structure, such as that shown in [20]. A distinct similarity with the picture in the left panel is noted.

crystals may be obtained with ease. These planar magnetic lattices with tunable lattice constants may present some potential applications, such as a modulation of surface waves and as a template for growing 2D photonic crystals.

[1] P. N. Pusey and W. van Megen, Nature (London) **320**, 340 (1986).

[2] A. D. Dinsmore, J. C. Crocker, and A. G. Yodth, Curr. Opin. Colloid Interface Sci. **3**, 5 (1998).

[3] Special issue on "From dynamics to devices: directed self-assembly of colloidal materials," edited by D. G. Grier [MRS Bull. **23**, No. 10, 21 (1998)].

[4] P. Yang, T. Deng, D. Zhao, P. Feng, D. Pine, B. F. Chmelka, G. M. Whitesides, and G. D. Stucky, Science **281**, 2244 (1998).

[5] A. V. Blaaderen, R. Ruel, and P. Wiltzius, Nature (London) **385**, 321 (1997).

[6] J. Zhu, M. Li, R. Rogers, W. Meyer, R. H. Ottewill, W. B. Russel, and P. M. Chaikin, Nature (London) **387**, 883 (1997).

[7] Z. Cheng, W. B. Russel, and P. M. Chaikin, Nature (London) **401**, 893 (1999).

[8] A. E. Larsen and D. G. Grier, Nature (London) **385**, 230 (1997).

[9] T. J. Chen, R. N. Zitter, and R. Tao, Phys. Rev. Lett. **68**, 255 (1992).

[10] L. Zhou, W. Wen, and P. Sheng, Phys. Rev. Lett. **81**, 1509 (1998).

[11] W. Wen, N. Wang, H. Ma, Z. Lin, W. Y. Tam, C. T. Chan, and P. Sheng, Phys. Rev. Lett. **82**, 4248 (1999).

[12] A. T. Skjeltorp, Phys. Rev. Lett. **51**, 2306 (1983); J. Appl. Phys. **55**, 2587 (1984).

[13] M. Golosovsky, Y. Saado, and D. Davidov, Appl. Phys. Lett. **75**, 4168 (1999).

[14] S. Yeh, M. Seul, and B. I. Shralman, Nature (London) **386**, 57 (1997).

[15] L. Ramos, T. C. Lubensky, N. Dan, P. Nelson, and D. A. Weitz, Science **286**, 2325 (1999).

[16] K. Zahn, R. Lenke, and G. Maret, Phys. Rev. Lett. **82**, 2721 (1999).

[17] C. Hammond, *The Basics of Crystallography and Diffraction* (Oxford University Press, New York, 1997).

[18] W. Y. Tam, G. H. Yi, W. Wen, H. Ma, M. M. T. Loy, and P. Sheng, Phys. Rev. Lett. **78**, 2987 (1997).

[19] We can use smaller microspheres than those used here. However, microspheres smaller than 1 μm in diameter are more difficult to coat and are also hard to control due to increased Brownian motion.

[20] C. Janot, *Quasicrystals, A Primer* (Clarendon Press, Oxford, 1992).